Red Blood Cell Abnormality Detection Under Federated Environment Using Deep Learning

Shakib Mahmud Dipto[1*†], Nadia Tasnim Mim[1], Md Tanzim Reza[1†], Md Sabbir Hossain[1], Md. Farhadul Islam[1] and Annajiat Alim Rasel[1]

[1*]Department of Computer Science and Engineering, BRAC University, Dhaka, Bangladesh.

*Corresponding author(s). E-mail(s): diptomahmud2@gmail.com;
Contributing authors: mimnadiatasnim@gmail.com;
md.sabbir.hossain1@g.bracu.ac.bd;
md.farhadul.islam@g.bracu.ac.bd; annajiat@gmail.com;
rezatanzim@gmail.com;
†These authors contributed equally to this work.

Abstract

Patients' concerns about their privacy lead many medical organizations to restrict access to their data. While protecting the confidentiality of the local data, Federated Learning (FL) may construct an unbiased global model by gathering updates from local models trained using the client's data. With the use of FL, this research hopes to solve the problem of centralized data collection by detecting deformations in images of red blood cells. Initially, multiple Deep Learning (DL) models were trained using the RBC data, and the highest-performing DL model was chosen for the FL model. It was trained using the model weights from the local model, which was done using the FL technique, but the client's data was kept private throughout the process. The results of the experiments indicate that there is no significant difference in the performance of the FL method and the best-performing DL Model since the best performing DL model reached an accuracy of 96% while the under FL environment it reached 94%. This research demonstrates that the FL technique, in comparison to the classic deep learning approach, can accomplish privacy-protected RBC deformation classification from RBC images without significantly reducing the accuracy of the classification.

Keywords: Federated Learning, VGG16, Red Blood Cell, deformations, Deep learning

1 Introduction

In medical case scenarios, many a time it is important to keep patient information confidential. Therefore, the use of a federated learning environment is beneficial in order to ensure data privacy. With the arrival of the pandemic Covid-19, various machine-learning algorithms have been used to detect the presence of the virus in patients' bodies. Hence, researchers used chest X-ray images to screen for Covid-19 using Federated learning [1]. The use of federated environments in medical cases can help in increasing the screening process by building powerful models. In their paper, the authors aimed for interpreting abnormalities in COVID-19 chest CT and conducted a multinational study on patients for external validation. They used a federated machine learning technique with help of Deep CNN and described its usability. For validation of the generalized model, they performed testing and training on 132 patients from three different hospitals as well as on independent datasets. The aim was to develop a useful AI in order to avoid aggregating mass amounts of data [2].

Deep learning models help us to increase the accuracy of our research. Therefore, in the medical field, using Deep Neural Networks to detect various disorders is an effective approach. The authors of this paper attempted to classify various types of cardiac disorders with the help of deep learning models. They proved the increase of accuracy in identifying the disorder with the help of deep learning models [3]. Researchers have performed and reviewed various machine learning techniques in order to increase the accuracy of abnormality detection to ensure security in IoT. They have suggested the use of Deep Learning models in order to increase the identification accuracy of possible security threats [4]. Deep learning models have been used for red blood cell abnormality detection in serious hematological disorders. Researchers have performed a vigorous investigation in order to detect anomalies in the blood cells of Sickle cell anemia patients. They proceeded to use the Alex Net deep learning model to detect 15 types of red blood cell shapes and achieved an impressive result which may help manage a patient life better by saving time [5].

With the increase of accuracy in the performance of models trained in federated environment, studies have been performed in medical cases such as Neurodevelopmental disorders like autism spectrum disorders. The study was performed on individuals in both behavioral and facial features. The authors have been successful in achieving better results with the help of models trained in federated environment[6]. The use of federated learning with neural networks for anomaly detection has been performed as well. The use of federated learning system ensures the security of the data. Moreover, it also facilitates low power consumption, lower latency as well as bandwidth. This research showed improvement in the prevention of theft during online transactions with

the model trained in a federated environment [7]. With the improvement of modern technology, malicious attempt at data stealing is a state of concern. The use of Federated Layer architectures (FLA) has been introduced in order to increase security in Medical Cyber-Physical Systems (MCPS) Networks in the process of model training. Furthermore, the use of FLA has been proven to have been helpful in the increased detection of the possibility of invasion within the MCPS environment [8].

As the Federated Learning system ensure the privacy of data as a decentralized technique, it has been used in intrusion detection system to provide security for internet-enabled devices as well. Moreover, research has been conducted on the aspects of anomaly detection using federated learning systems with ML techniques and also the challenges have been discussed [9]. Red blood cell abnormalities are common in many medical emergencies. Often times it can be an early sign of clinical deterioration of health in serious medical cases like Sepsis [10]. Another study on Sickle cell anemia patients' red blood cell classification used a deep learning model as well. The authors proceeded to use several data augmentation techniques and transfer learning and introduced a model that produced noteworthy performance in Microscopy images [11]. The use of deep learning to diagnose blood cells can aid in identifying various blood-related diseases. A deep learning model has been proposed to help to detect blood cell diseases and achieved a noteworthy accuracy rate [12]. Red blood cell classification can help in identifying various blood cell-related diseases. The use of deep learning models has been able to achieve better results in large datasets [13]. Automated machine learning method to identify abnormal red blood cells utilizes to advantages of machine learning and increases the detection capacity [14].

In this study, the FL method was used to classify RBC anomalies from RBC images. The client information was hidden and no information was shared while training the FL model. The dataset was divided into 7:2:1 ratios for training, validation, and evaluation purposes of the DL model. The best-performing DL model was selected for training the FL model. The client's data was not shared while training the FL Method. Finally, the accuracy rate was compared for both the DL model and the FL model.

The rest of the paper consists of the following sections. Section 2 contains the description of the proposed methodology. Section 3 includes the result analysis of this experiment. Finally, the paper is concluded in Section 4.

2 Proposed Model

The study's methodology consisted of two primary parts, each dedicated to the detection of RBC abnormalities. The two primary parts of our proposed methodology are depicted in Figures 1 and 2, respectively.

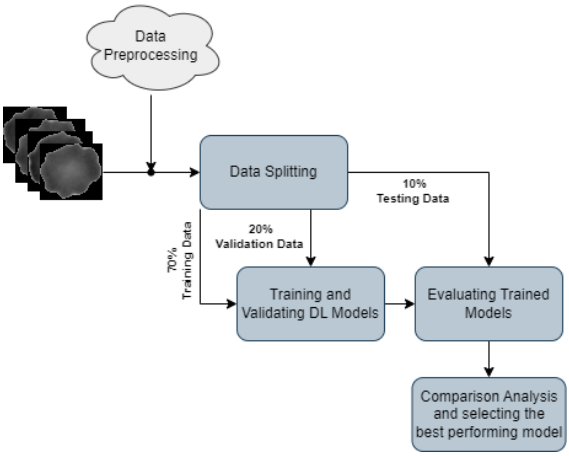

Fig. 1: The steps that were taken to find the DL model that was the most effective in identifying RBC abnormalities were included in the suggested system.

The steps toward identifying the most effective DL model for RBC abnormality classification are depicted in Fig. 1. The first step was to get the data from the original source and preprocess it. As part of the preprocessing, we normalized the RBC images with Principal Component Analysis (PCA) and downsampled them to a resolution of 128x128 pixels. Next, we made a 7:2:1 split of our collected data. 70% of the image was picked randomly for training the models, 20% was utilized for validation, and the remaining 10% was used for the evaluation process. We have trained and compared the performance of three DL models (VGG19, ResNet50, and Inception v3).

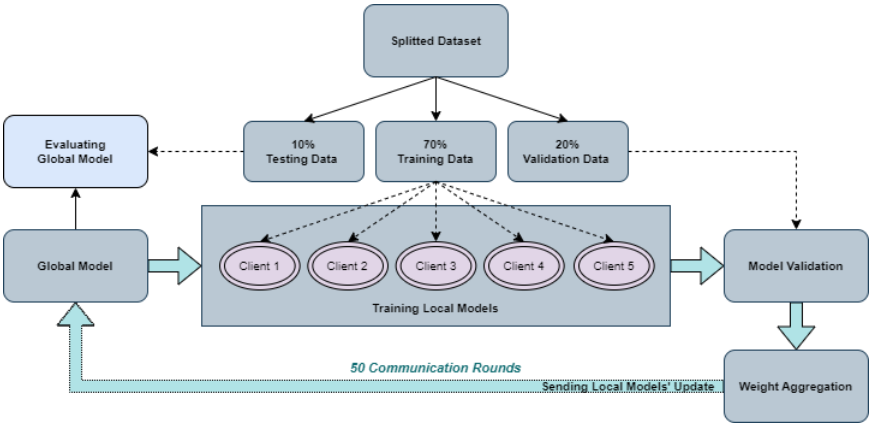

Fig. 2: The proposed method for identifying RBC abnormalities under FL environment by employing DL model

After identifying the DL model with the highest performance, we used it to build the global model. After that, we made five local versions of the global model. We used our split dataset and gave each of our five clients their own unique training data as well as their own local model. We used our split dataset and distributed a random number of unique training data and a local model to each of the five clients. After that, the clients trained the local models by utilizing the given data, and the model validation was carried out utilizing the validation dataset. Following the training and validation of the local models, the aggregated trained weights of the local models were calculated. After that, the aggregated weight was sent to the global model during each cycle of communication. This training was carried out for a total of fifty rounds of communication. After finishing the training, we evaluated the performance of the global model by utilizing the testing dataset.

2.1 Description of the Dataset

The dataset used in this study is available on Mendeley Data [15] and is referred to as RBCdataset. The RBC dataset consists of a total of 7,108 RBC images, all of which have been obtained from nine separate classes. Fig. 3 illustrates a classwise breakdown of the data contained in the RBC dataset. It has come to our attention that the Pencil class only has a total of 24 images. Therefore, we skipped that class entirely and utilized the images from the remaining eight classes to train and evaluate our models.

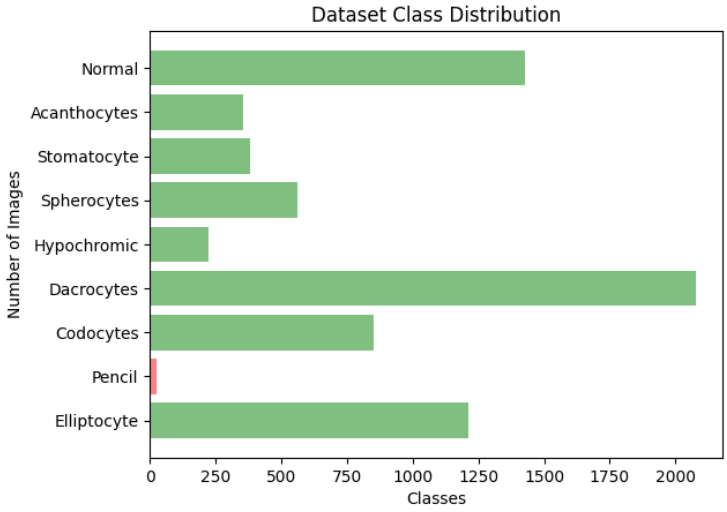

Fig. 3: Class Distribution of the RBCdataset

The eight classes include Elliptocytes, Dacrocytes, Acanthocytes, Stomatocytes, Spherocytes, Hypochromic, Codocytes, and Normal. Elliptocyte are known for their pencil-shaped structure. At the time of circulation fully-grown

RBCs encounter stress and thus they generate Elliptocytes [16, 17]. Under normal circumstances, RBCs in general contains a really low number of elliptocytes. Dacrocytes are of tear-drop shape. RBCs take this form when it gets affected in its bone marrow with cancer such as Metastatic. Acanthocytes is the sign of iron deficiency [18]. Stomatocytes generate due to the severe swelling that replaces the central zone of RBC with an incision-like cut [19]. The sphere like shaped RBCs are known as Spherocytes. Hereditary spherocytosis and anemia cause RBCs to lose their biconcave, circular structure and takes upon the form of a sphere [20]. Hypochromic cells refer o iron deficiency. It is a result of low hemoglobin in RBCs [21]. Codocytes mass produces when there is a chance of liver diseases. It is also known as target cell due to its appearance as a target practice for shooting with a bulls eye [20]. Normal RBCs represent healthy cells with a typical round shape. Sample distribution of the classes is given in Fig. 4.

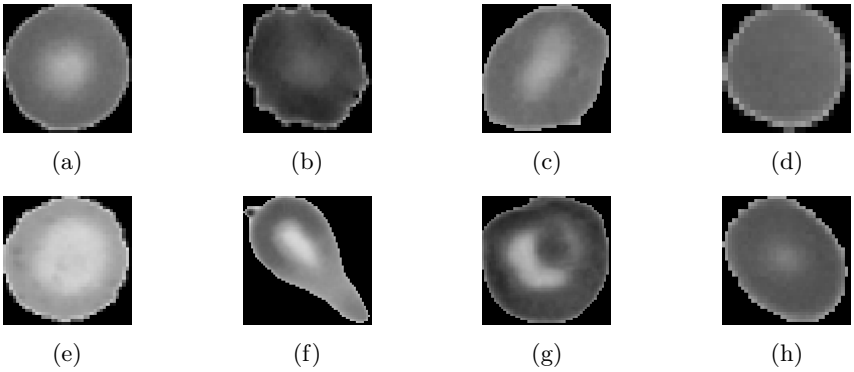

Fig. 4: Sample Data of RBCdataset. (a) Normal, (b) Acanthocytes, (c) Stomatocytes, (d) Spherocytes, (e) Hypochromic, (f) Dacrocytes, (g) Codocytes, (h) Elliptocyte

2.2 Deep Learning Architecture

In the proposed system, we utilized the TensorFlow [22] and Keras [23] libraries to implement the VGG16, ResNet50, and Inception V3 architectures. We were able to obtain quicker training convergence by making use of the weights that had been learned earlier on the ImageNet database [24]. The convolution layers were preserved as the default architecture. However, we dropped the fully connected layers. After that, a flattened layer was added, and the output was then sent to a dense layer that had 1024 neurons. Following that, a 50% dropout layer was added to prevent overfitting by randomly eliminating half of the neuron connections from our model during each training cycle. The ReLU activation function was utilized for the dense layers, meanwhile, the softmax activation function was utilized for the output layer. In addition

to that, we made use of Adam Optimizer and set the learning rate to 0.00001. The architecture of the DL models that we employed is depicted in Fig. 5.

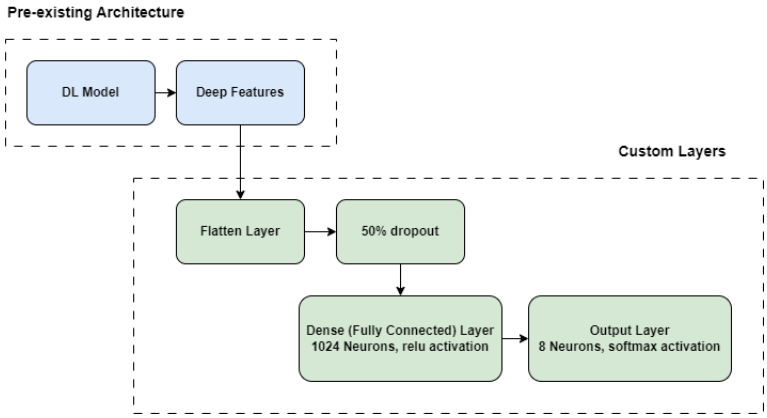

Fig. 5: Architecture of the Used Deep Learning Models

2.3 Model Training

The labeled data were used to train the DL models, and these data were classified into eight distinct groups. Keras and Tensorflow 2.6.0 were utilized in the construction of the model, and an RTX 3090 was chosen as the GPU for the experimental setup. In order to train our model to make use of transfer learning while utilizing the default architecture, the image sizes were reduced to 128 × 128. The DL model functions more effectively with a balanced dataset, although the dataset that was used had certain imbalances.

$$Weight_{class} = \frac{Total\ Number\ of\ Training\ Image}{Number\ of\ trainingimage\ from\ class \times Number\ of\ class} \tag{1}$$

Consequently, throughout the training session, significantly uneven weights were assigned to each image of any particular class. Following the completion of the computation, the 'Hypochromic' class was found to have the most significant weight of 2.79, while the 'Dacrocytes' class was found to have the lowest weight of 0.3. The formula for assigning weights is described in equation 1, and the weight that was computed for each class is shown in table 1. The batch size for the model training was thirty-two, and there were a total of fifty epochs used. Immediately following the completion of the model training, each of the models was kept separately for use in further experiments.

Class of RBCdataset	Calculated Weights
Elliptocyte	0.5118
Codocytes	0.7283
Dacrocytes	0.2985
Hypochromic	2.7917
Spherocytes	1.1008
Stomatocyte	1.6224
Acanthocytes	1.7507
Normal	0.4346

Table 1: Weights for the Classes of RBCdataset

2.4 Model Validation

The validation set, which contains 20% of the data, was used to evaluate how well the models performed. During the process of training the models, it was necessary to make an evaluation of how well the model was progressing with each iteration. Therefore, based on the data that was not observed, our experimental models were able to determine the accuracy of the RBC abnormality detection utilizing prior knowledge and experience. The effectiveness of the models was evaluated with respect to their level of accuracy. If validation wasn't done, there is a good likelihood that the results that were obtained after training were skewed.

2.5 Model Testing

We do an optimization of the hyperparameters by basing it on the observations made on the validation set. As a result, there is a chance that the model will become skewed in favor of the validation data. After the training phase of the model has been completed, it is essential to evaluate the model using a different set of data. As a result, we have set aside 10% of the data included in the RBC dataset to use as a test set. This 10% of the data was utilized in the evaluation of the predictions that were produced by the trained models. Our trained models were able to estimate the RBC abnormality by applying their existing knowledge and expertise based on the data that was not experienced.

2.6 Federated Learning (FL)

Federated Learning (FL) is a machine learning method that addresses the complications of rigorous rules due to data privacy and sparse resource of datasets availability [25–27]. Federated Learning consists of two edges. The first one is known as the global server or central server. The central server consists of a global model. The second one is the local server which is also known as the client end. The client-server accommodates the local data stored by clients on their terminal appliances. FL method facilitates model training without any transfer of information. This method trains the model on several segregated endpoint devices. These devices contain the information, stationed in the local servers. The local model is trained on the client dataset and then sends the updated weights to the global model. Thus the expected security and

privacy in medical data prognosis are maintained by the FL method [28–30]. Fig. 6 illustrates an overview of the Federated Learning architecture.

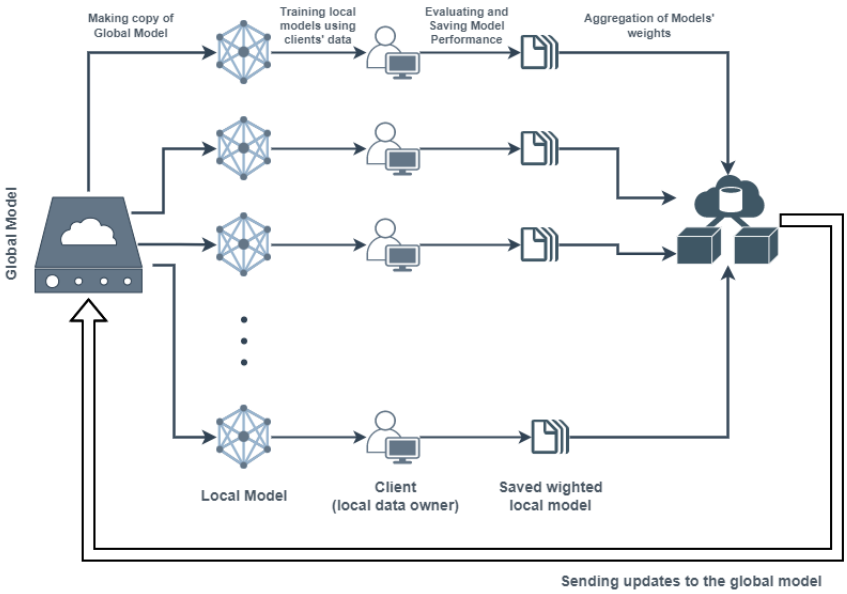

Fig. 6: Architecture of Federated Learning (FL) Environment

3 Experimental Result Analysis

The subsequent part contains the final findings of our implementation as well as an evaluation of how well our models function to identify RBC abnormalities. For each model that was attempted, the values for precision, recall, F1 score, confusion matrix, AUC score, ROC curve, accuracy, and loss function are shown. The equation **??** demonstrates the many formulae that are used to compute accuracy, precision, recall, f1-score, and specificity. Our key objective was to get a greater test accuracy while simultaneously reducing the amount of model loss function. Every model was executed for a total of fifty epochs using Adam as the optimizer and setting the learning rate to 0.00001. Following the training, the best-performing DL model was selected to become the global model based on the values obtained from the results. Then we train it in an FL environment. Overall, we summarized our efforts by making comparisons to other state-of-the-art methods that have been previously published.

$$Accuracy = \frac{TP + TN}{TP + TN + FP + FN} \tag{2}$$

$$Precision = \frac{TP}{TP + FP} \tag{3}$$

$$Recall = \frac{TP}{TP + FN} \tag{4}$$

$$f1 - score = \frac{2 * TP}{2 * TP + FP + FN} \tag{5}$$

$$Specificity = \frac{TN}{TN + FP} \tag{6}$$

3.1 Performance Evaluation of DL Models

We trained VGG16, Inception v3, and ResNet50 models for 50 epochs each. The accuracy and the loss curves for the models are given in the following figure:

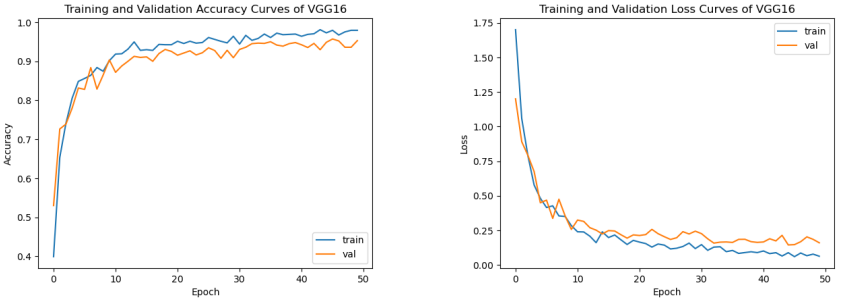

Fig. 7: VGG16 Accuracy and Loss Curve

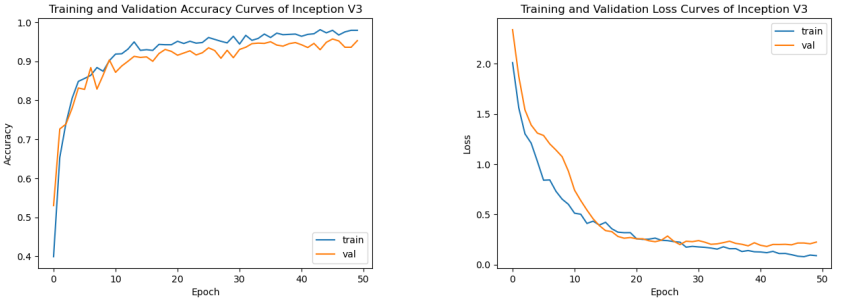

Fig. 8: Inception v3 Accuracy and Loss Curve

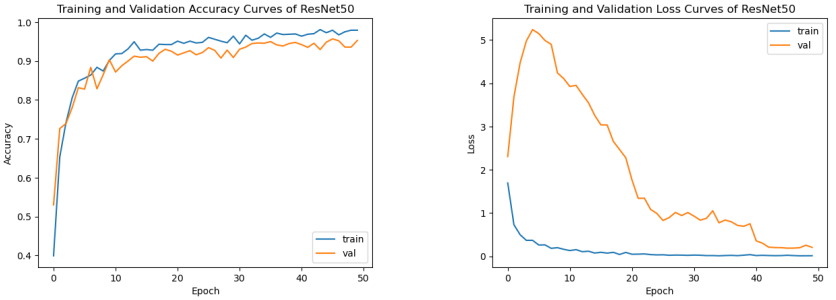

Fig. 9: ResNet50 Accuracy and Loss Curve

If we follow the training pattern of the three models, we can see that all the models reach near their peak training scores at around 20 epochs. The training accuracy and loss patterns for Inception v3 and VGG16 showcases smooth pattern, representing proper learning without any issues. Meanwhile, the validation loss curve for ResNet50 architecture showcases a large spike at the beginning, which is likely caused by overstepping local minima due to a larger than necessary learning rate. However, the model gradually rectifies it as the training goes on. Except for ResNet, all other models' training and validation accuracy-loss curves run smoothly side by side; no abnormality was seen. In 10, the classification results for the three models are given.

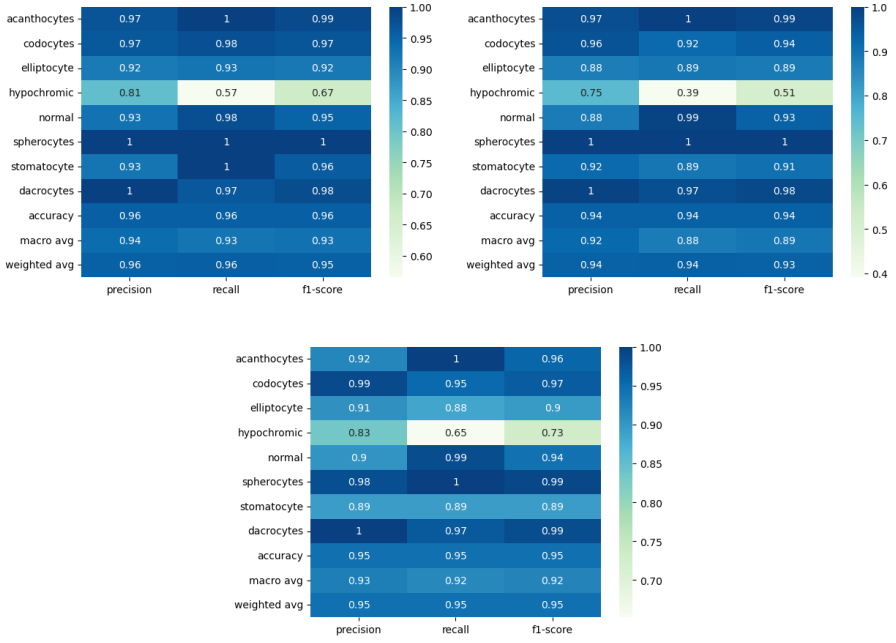

Fig. 10: Classification reports of the models

A common pattern of not being able to classify the hypochromic RBC images is present in the classification reports, as the precision, recall, and the f1-score are low for that class. The failure of classifying the hypochromic RBC images is also evident in the confusion matrices given in Fig. 11.

As visible in Fig. 11, the shortage of samples in the hypochromic RBC image class makes it difficult for the models to classify them properly. Regardless, the ResNet model still manages to classify them fairly accurately. The prediction accuracy for all the other classes is satisfactory for all the other classes, as visible in Fig. 10.

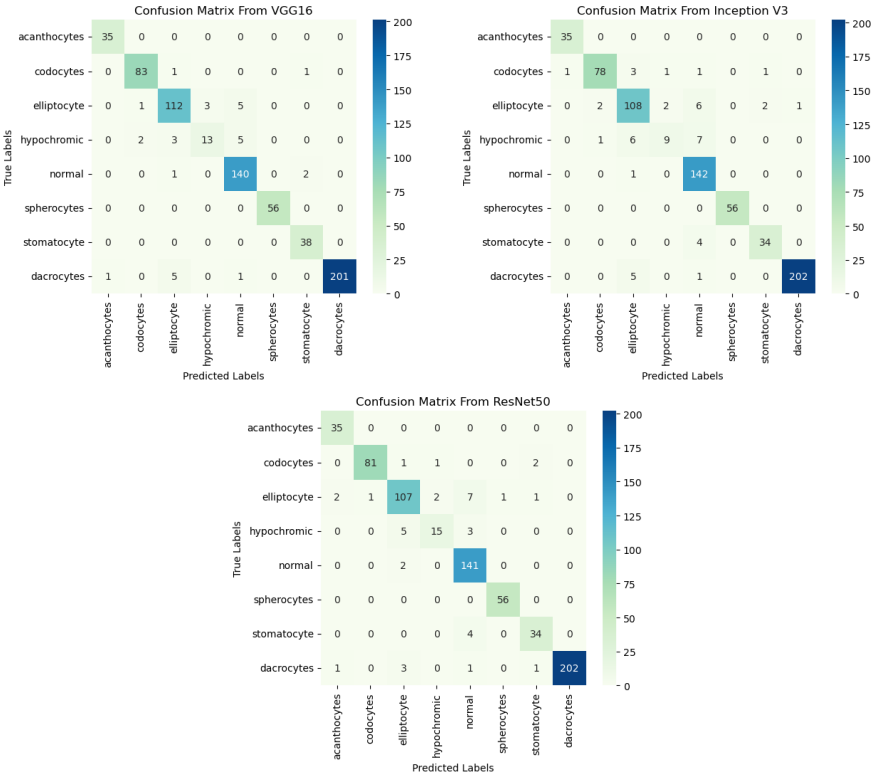

Fig. 11: Confusion matrices of the models

Among the three models, the VGG16 model comes to the top with 96% overall accuracy across all the classes. Consequently, VGG16 turned out to be our preferred model for the FL environment.

Afterward, we analyzed the ROC curve and the AUC score of the models. The analyzed ROC curves are given in Fig. 12. The models achieved the perfect AUC score for the acanthocyte class and the lowest AUC score for the hypochromic class. Apart from the hypochromic class, a satisfactory AUC score was achieved for all the other classes across all the models.

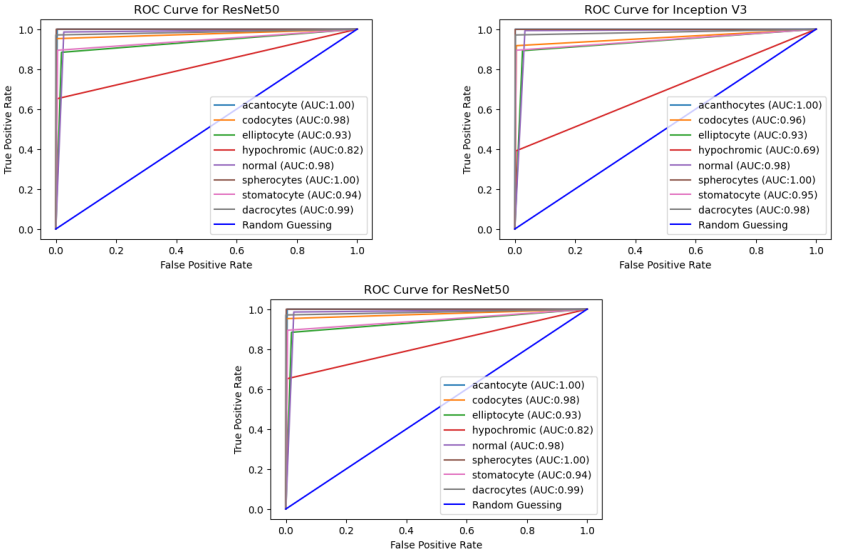

Fig. 12: ROC curve of the models

3.2 Performance Evaluation of Federated Learning

In the process of creating the FL environment, we divided the data into five segments, each segment representing a single client. A separate test set was also kept to analyze the testing performance of the federated global model. The FL simulation was run for 50 communication rounds, where each communication round represents one epoch on each client's dataset.

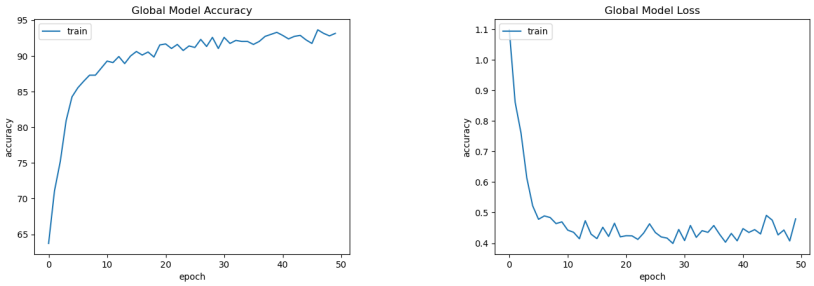

Fig. 13: Federated Learning Global Model Accuracy and Loss Curve

The global accuracy and loss curve across the communication rounds visualizes a healthy rate of changes. The accuracy quickly increased until the 15th communication round and then gradually increased with occasional spikes until the 50th communication round. Both the accuracy and the loss curves reached

a plateau after the 50th round so we decided to keep the record until that point.

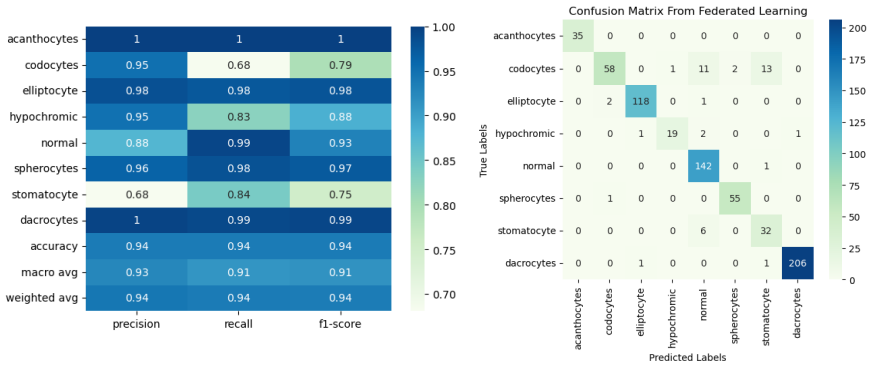

Fig. 14: Federated Learning Classification Report and Confusion Matrix

Surprisingly, as evident in Fig. 14, while the FL global model performs well on the non-hypochromic RBC image classes like the centrally trained models, it also performs well to classify the hypochromic RBC images, something that the centrally trained models failed to achieve. In the centralized environment, the models failed to properly classify the hypochromic RBC images due to the low number of samples. Meanwhile, in the FL environment, the VGG model had to work on a non-IID dataset due to the nature of the environment, which likely led the model to work well on classes with low sample distribution. The ROC curve for the global model under the FL environment is given in 15. As mentioned previously, FL seems to solve the issue of classifying hypochromic classes accurately, with a 0.91 AUC score for the corresponding class. Meanwhile, a lower AUC score was achieved for the codocyte class compared to the centrally trained models. Apart from the mentioned two classes, a balanced AUC score was maintained across the central and decentralized models.

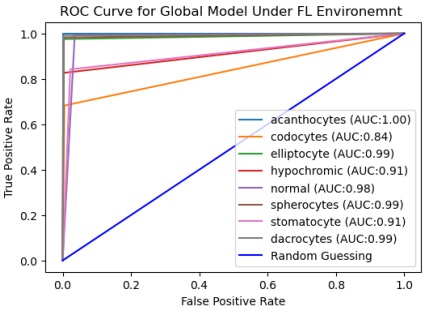

Fig. 15: ROC curve for FL global model

Overall, under the federated setting, the VGG16 model managed to score an accuracy of 94%, which is quite close to the 96% accuracy score achieved by the centrally learned VGG16 model. This demonstrates the fact that even under the FL setting, it is possible to classify RBC deformation nearly as accurately as in the normal setting. In FL, there was a sacrifice of only 2% accuracy score with a better distribution of precision and recall scores across the classes. As the FL environment ensures data privacy and provides opportunities for open-source training integration, the added benefits are huge. Therefore, a decrease of 2% accuracy score is a worthy trade-off from our point of view. This research thus proves the effectiveness of FL for the classification of RBC image data.

Finally, we compared our FL approach to the State Of The Art (SOTA) result from another paper on the same dataset.

Table 2: Comparison Against Literature

	Sensitivity (%)		**Specificity (%)**	
Classes	**Literature**	**Proposed**	**Literature**	**Proposed**
acanthocyte	97.84	100.00	99.71	100.00
codocyte	88.38	99.52	98.73	68.24
elliptocyte	98.10	99.66	99.57	97.52
hypochromic	94.97	99.85	99.52	82.61
normal	91.75	96.47	98.16	99.30
spherpcyte	94.83	99.69	98.12	98.21
stomatocyte	88.94	97.76	99.12	84.21
dacrocyte	100.00	99.80	99.78	99.04

From 2, we can say that the proposed FL architecture conclusively achieved better sensitivity across most of the classes. Meanwhile, the specificity scores across the classes are generally lower compared to the literature. With a better sensitivity score, the proposed FL architecture should be able to detect a particular RBC deformation type fairly well. Additionally, the overall accuracy score for both the literature and the proposed FL architecture is 94%, showcasing the prevalence of the FL system. Even with e decentralized learning structure, FL performs quite competitively against models from the literature.

4 Conclusion

Restricted access to datasets of patients due to their privacy and security concerns makes it hard for researchers to obtain medical-related datasets and work with ML models due to insufficient data. The use of the Federated Learning model aids in conserving the confidentiality of clients' data and preparing an unbiased global model. This research work aims to generate a solution for the centralized data collection problem in red blood cell images using FL. This work used multiple Deep Learning models like VGG19, ResNet50, and Inception v3 in order to train the RBC data. The dataset was initially split into a

7:2:1 ratio. The DL models were trained using 70% data of the dataset and then 20% of the dataset was used for validation. Finally, the remaining 10% of the data was used for evaluation purposes. The best-performing DL model VGG16 which achieved an accuracy rate of 94% was elected for the FL model. FL technique was implemented to train the DL model using model weights from the local model. The clients' data was kept private throughout the process of training the FL model. The trained FL model obtained 96% accuracy rate all the while maintaining the confidentiality of clients. Moreover, the outcome of this experiment shows that both FL method and DL method provides similar performance as the achieved accuracy for detecting RBC anomalies was the same for both model. Furthermore, it can be concluded that this study denotes that the FL technique can protect the client's data and detect RBC abnormalities from RBC images in contrast to the traditional deep learning approach while consistently maintaining the accuracy of the classification.

References

[1] Feki, I., Ammar, S., Kessentini, Y., Muhammad, K. (2021). Federated learning for COVID-19 screening from Chest X-ray images. Applied Soft Computing, 106, 107330.

[2] Dou, Q., So, T. Y., Jiang, M., Liu, Q., Vardhanabhuti, V., Kaissis, G., ... Heng, P. A. (2021). Federated deep learning for detecting COVID-19 lung abnormalities in CT: a privacy-preserving multinational validation study. NPJ digital medicine, 4(1), 1-11.

[3] Khan, A. H., Hussain, M., Malik, M. K. (2021). Cardiac disorder classification by electrocardiogram sensing using deep neural network. Complexity, 2021.

[4] Sharma, B., Sharma, L., Lal, C. (2019, December). Anomaly detection techniques using deep learning in IoT: a survey. In 2019 International conference on computational intelligence and knowledge economy (ICCIKE) (pp. 146-149). IEEE.

[5] Aliyu, H. A., Razak, M. A. A., Sudirman, R., Ramli, N. (2020). A deep learning AlexNet model for classification of red blood cells in sickle cell anemia. Int J Artif Intell, 9(2), 221-228.

[6] Shamseddine, H., Otoum, S., Mourad, A. (2022). A Federated Learning Scheme for Neuro-developmental Disorders: Multi-Aspect ASD Detection. arXiv preprint arXiv:2211.00643.

[7] Singh, S., Bhardwaj, S., Pandey, H., Beniwal, G. (2021). Anomaly detection using federated learning. In Proceedings of International Conference on Artificial Intelligence and Applications (pp. 141-148). Springer, Singapore.

[8] Siniosoglou, I., Sarigiannidis, P., Argyriou, V., Lagkas, T., Goudos, S. K., Poveda, M. (2021, June). Federated intrusion detection in NG-IoT healthcare systems: An adversarial approach. In ICC 2021-IEEE International Conference on Communications (pp. 1-6). IEEE.

[9] Agrawal, S., Sarkar, S., Aouedi, O., Yenduri, G., Piamrat, K., Alazab, M., ... Gadekallu, T. R. (2022). Federated learning for intrusion detection system: Concepts, challenges and future directions. Computer Communications.

[10] Ko, E., Youn, J. M., Park, H. S., Song, M., Koh, K. H. (2018). Early red blood cell abnormalities as a clinical variable in sepsis diagnosis. Clinical Hemorheology and Microcirculation, 70(3), 355-363.

[11] Alzubaidi, L., Fadhel, M. A., Al-Shamma, O., Zhang, J., Duan, Y. (2020). Deep learning models for classification of red blood cells in microscopy images to aid in sickle cell anemia diagnosis. Electronics, 9(3), 427.

[12] Khalil, A. J., Abu-Naser, S. S. (2022). Diagnosis of Blood Cells Using Deep Learning. International Journal of Academic Engineering Research (IJAER), 6(2).

[13] Aliyu, H. A., Sudirman, R., Razak, M. A. A., Abd Wahab, M. A. (2018, July). Red blood cell classification: deep learning architecture versus support vector machine. In 2018 2nd international conference on biosignal analysis, processing and systems (ICBAPS) (pp. 142-147). IEEE.

[14] Wong, A., Anantrasirichai, N., Chalidabhongse, T. H., Palasuwan, D., Palasuwan, A., Bull, D. (2021). Analysis of Vision-based Abnormal Red Blood Cell Classification. arXiv preprint arXiv:2106.00389.

[15] Tyas, D. A., Ratnaningsih, T., Harjoko, A., Hartati, S. (2022). Erythrocyte (red blood cell) dataset in thalassemia case. Data in Brief, 41, 107886.

[16] Landis-Piwowar, K., Landis, J., Keila, P. (2015). The complete blood count and peripheral blood smear evaluation. Clinical laboratory hematology. 3rd ed. New Jersey: Pearson, 154-77.

[17] Manchanda, N. (2015). Anemias: red blood morphology and approach to diagnosis. Rodak's hematology clinical applications and principles. 5th ed. St. Louis, Missouri: Saunders, 284-96.

[18] Bosman, G. J. (2018). Disturbed red blood cell structure and function: an exploration of the role of red blood cells in neurodegeneration. Frontiers in Medicine, 5, 198.

[19] Andolfo, I., Russo, R., Gambale, A., Iolascon, A. (2018). Hereditary stomatocytosis: an underdiagnosed condition. American journal of hematology, 93(1), 107-121.

[20] Parab, M. A., Mehendale, N. D. (2021). Red blood cell classification using image processing and CNN. SN Computer Science, 2(2), 1-10.

[21] Dinh, N. H., Cheanh Beaupha, S. M., Tran, L. T. A. (2020). The validity of reticulocyte hemoglobin content and percentage of hypochromic red blood cells for screening iron-deficiency anemia among patients with end-stage renal disease: a retrospective analysis. BMC nephrology, 21(1), 1-7.

[22] Abadi, M., Agarwal, A., Barham, P., Brevdo, E., Chen, Z., Citro, C., ... Zheng, X. (2016). Tensorflow: Large-scale machine learning on heterogeneous distributed systems. arXiv preprint arXiv:1603.04467.

[23] Chollet, F., & others. (2015). Keras. GitHub. Retrieved from https://github.com/fchollet/keras.

[24] Deng, J., Dong, W., Socher, R., Li, L. J., Li, K., Fei-Fei, L. (2009, June). Imagenet: A large-scale hierarchical image database. In 2009 IEEE conference on computer vision and pattern recognition (pp. 248-255). Ieee.

[25] Aledhari, M., Razzak, R., Parizi, R. M., Saeed, F. (2020). Federated learning: A survey on enabling technologies, protocols, and applications. IEEE Access, 8, 140699-140725.

[26] Zhang W, Lu Q, Yu Q, Li Z, Liu Y, Lo SK, Chen S, Xu X, Zhu L (2020) Blockchain-based federated learning for device failure detection in industrial iot. IEEE Internet Things J 8(7):5926–5937.

[27] Sarma KV, Harmon S, Sanford T, Roth HR, Xu Z, Tetreault J, Xu D, Flores MG, Raman AG, Kulkarni R et al (2021) Federated learning improves site performance in multicenter deep learning without data sharing. J Am Med Inform Assoc 28(6):1259–1264.

[28] Zhang W, Zhou T, Lu Q, Wang X, Zhu C, Wang Z, Wang F (2020) Dynamic fusion based federated learning for covid-19 detection. arXiv:2009.10401.

[29] Aich S, Sinai NK, Kumar S, Ali M, Choi YR, Joo M-I, Kim H-C (2021) Protecting personal healthcare record using blockchain & federated learning technologies. IEEE, pp 109–112.

[30] Stripelis D, Ambite JL, Lam P, Thompson P (2021) Scaling neuroscience research using federated learning. IEEE, pp 1191–1195.